Vol. 17, No. 3 (2018) 847-861
Revista Mexicana de Ingeniería Química

MICROPOROUS ACTIVATION CARBON MADE OF SAWDUST FROM TWO FORESTRY SPECIES FOR ADSORPTION OF METHYLENE BLUE AND HEAVY METALS IN AQUEOUS SYSTEM - CASE OF REAL POLLUTED WATER

CARBÓN ACTIVADO MICROPOROSO PRODUCIDO DE ASERRÍN DE DOS ESPECIES FORESTALES PARA LA ADSORCIÓN DE AZUL DE METILENO Y METALES PESADOS EN MEDIO ACUOSO - CASO AGUA DE RÍO CONTAMINADA

J.F. Cruz[1], G.J.F. Cruz[1*], K. Ainassaari[3], M.M. Gómez[4], J.L. Solís[4], R.L. Keiski[3]

[1] *Universidad Nacional de Piura, Departamento de Química, Campus Universitario s/n Miraflores, Piura, Perú.*
[2] *Universidad Nacional de Tumbes, Departamento de Ingeniería Forestal y Gestión Ambiental, Av. Universitaria s/n, Campus Universitario - Pampa Grande, Tumbes, Perú.*
[3] *University of Oulu, Faculty of Technology, Environmental and Chemical Engineering, P.O.Box 4300, FI-90014 University of Oulu, Finland.*
[4] *Universidad Nacional de Ingeniería, Facultad de Ciencias, Av. Túpac Amaru 210, Lima 25, Perú.*

Received February 5, 2018; Accepted April 4, 2018

Abstract

Activated carbon samples were prepared and characterized from two novel forestry precursors by one-step chemical activation with $ZnCl_2$. The adsorption capacities of the adsorbents were tested with methylene blue in monocomponent synthetic solution and with heavy metals from polluted river water. The specific surface areas (S_{BET}) of the produced activated carbons were 1278 and 1404 m^2/g. Further characterization was carried out by FTIR, RAMAN spectroscopy, XRD and FESEM analysis. The pore structure of both activated carbons was predominantly microporous with presence of mesopores. The maximum methylene blue (MB) adsorption capacities for both activated carbons were 250 mg/g and 357 mg/g. MB kinetic experiments were carried out and the influence of the initial MB concentration and the activated carbon dosage was evaluated. The samples reached removal levels close to 100% during the first 5 min of experiments with dissolved As(V) and Pb(II) in the polluted river water, reducing the concentration of these elements until levels below the local water quality standards.

Keywords: sawdust, adsorption, methylene blue, heavy metals, aqueous system.

Resumen

Se prepararon carbones activados a partir de dos precursores de la actividad forestal utilizando activación química en un solo paso con $ZnCl_2$. Las capacidades de adsorción se determinaron con azul de metileno en soluciones sintéticas y con metales pesados de agua de un río contaminado. Las áreas superficiales específicas de los carbones activados se calcularon entre 1278 y 1404 m^2/g. Una caracterización de los materiales se realizó mediante FTIR, espectroscopía RAMAN, difracción de rayos X y microscopía electrónica de barrido. La estructura porosa de ambos carbones activados fue predominantemente microporosa con presencia de mesoporos. La máxima adsorción de azul de metileno por ambos carbones fue de entre 250 mg/g y 357 mg/g. La cinética de adsorción de azul de metileno con diferentes concentraciones iniciales del colorante y diferentes dosis de carbón activado, también fue evaluada. Las muestras alcanzaron una capacidad de remoción de As(V) y Pb(II) disueltos en agua de un río contaminado cercanas 100 % durante los primeros 5 min, reduciendo los valores de estos contaminantes a niveles por debajo de los estándares de calidad de agua locales.

Palabras clave: aserrín, adsorción, azul de metileno, metales pesados, sistemas acuosos.

* *Corresponding author. E-mail*: gcruzc@untumbes.edu.pe

1 Introduction

Forestry industry is an important activity in Peru. Different forestry species are extracted from Peruvian forest to be processed for a wide range of applications. *Cedrelinga catenaeformis Ducke* is a specie extracted from the rainforest in Peru and Ecuador and it is widely used for furniture, doors and windows manufacture. *Colicodendron scabrida* (*Capparis scabrida*) is a specie from the dry forest used to produce handicraft in northwest of Peru.

In the productive activities associated with both species, a significant amount of residues is generated. The main residue is sawdust, which is stored and accumulated in the factories and workshops. Currently, this biomass is used as an energy source for brick production; however, different gases (CO_2, CO, etc.) and particles are released to the atmosphere by the small-scale ovens used for this aim. In other cases the sawdust is just thrown away in illegal dumps generating environmental detriment.

Nowadays one of the main concerns in the activated carbon production is the possibility to replace coal, the traditional precursor in the activated carbon preparation, by other inexpensive renewable raw materials. Sawdust and other forestry byproducts have been used as starting materials for activated carbon production and their application in the removal of pollutants in aqueous phase such as rattan sawdust (Hameed *et al*., 2007a), *Hevea brasiliensis*, commonly named rubber wood sawdust (Karthikeyan *et al*., 2004; Srinivasakannan and Bakar, 2004), wood apple shell (Malarvizhi and Sulochana, 2008), *Ceiba petandra* hulls (Rao *et al*., 2006), teak sawdust (Ismadji *et al*., 2005), Bamboo (Hameed *et al*., 2007b; Velázquez-Trujillo *et al*., 2010), and *Tectona grandis* sawdust (Mohanty *et al*., 2005) among others.

Water pollution is a worldwide concern, and dyes and heavy metals are two of the most common and dangerous pollutants for the natural ecosystems. Dyes are widely used in textile factories and they are disposed in the wastewater in rivers and other water bodies, causing negative effects over the fauna, flora and even humans. Methylene blue is one of the most used dyes in an industrial scale and it has been commonly used as an organic pollutant model to evaluate the adsorption capacity of activated carbons and others adsorbents.

It is common to find polluted rivers by heavy metals and metalloids in many developing countries, particularly at areas where the basins are influenced by mining activities. Mining activities could produce wastewater with pollutants such as As, Pb, Hg, among others; and they end up in the natural water streams especially from illegal mining activities when the competent governmental officers cannot deal with the applications of the laws. One example of these cases takes place in the Tumbes river (northwest Peru) where illegal small-scale gold mining, located in Ecuador (where the river has its origin), pollutes the water mainly with As and Pb. These pollutants affect significantly the aquatic ecosystem and reduce the water quality. Thus, the inhabitants live in rural areas surrounding to the river are exposed to this polluting load. In that framework is still important to find new low cost, abundant and renewable raw materials for activated carbon production with well-developed porous structure. Most of adsorption experiments have been carried out using synthetic solution of the tested pollutant instead of multicomponent real polluted water. Therefore, the aims of the present research are (i) to produce and characterized high quality microporous activated carbons from two novel precursors *Cedrelinga catenaeformis Ducke* and *Colicodendron scabrida* sawdust based on one-step activation; (ii) to test the adsorption capacity of the adsorbents with methylene blue as organic pollutant model from a single synthetic aqueous system; and (iii) to test the As and Pb adsorption capacity of the adsorbents from a sample of real polluted river water.

2 Methods

2.1 Production of activated carbon

Sawdust from two forestry species *Cedrelinga catenaeformis Ducke* and *Colicodendron scabrida* was collected from different workshops in the northwest of Peru. The samples were dried, ground and sieved to obtain the fraction with particle size between 0.5 and 1 mm. The activation and carbonization were carried out in a single step (Cruz *et al*., 2012; Cruz *et al*., 2015). The precursors were mixed exhaustively with $ZnCl_2$ (Emsure ACS, ISO, Reag. Ph Eur - Merck) in similar weight proportion in aqueous media at room temperature. The mixture was immediately put in a ceramic crucible and then in a horizontal oven to be directly activated-carbonized. The temperature of the oven was increased at a rate of 10 °C/min, until it reached the final carbonization temperature of 600

°C. The carbonization and activation process took 2 h and then the samples were cooled. The whole process occurred under nitrogen atmosphere (150 ml/min). The carbonized material was washed with a solution of HCl (0.15 M) and then repeatedly washed with hot and room temperature distilled water. Finally, the samples were dried overnight, grounded and sieved to obtain particle size lower than 0.25 mm and between 0.25 and 0.5 mm.

Activated carbon samples were codified with codes CCs and CSs for *Cedrelinga catenaeformis Ducke* and *Colicodendron scabrida*, respectively.

2.2 Characterization of activated carbons

The calculation of textural parameters was based on the information of the nitrogen physisorption isotherms measured by a surface area and porosity analyzer Micromeritics ASAP 2020 (Micromeritics, USA). Specific surface area (S_{BET}) was calculated via the classical Brunauer-Emmett-Teller (BET) theory using the values of relative pressure (p/p0) in the range between 0.05-0.25 (Brunauer *et al*., 1938), taking into account a positive slope of the BET model curve. The total pore volume (V_{net}) was determined using the data of nitrogen adsorption at the maximum value of p/p_0 (~0.9900) from the adsorption branch. The micropore volume was determined via Dubinin-Radushkevich equation (V_{DR}) considering N_2 adsorption data at relative pressure lower than 0.1. The N_2 volume adsorbed at relative pressure close to 0.10 ($V_{0.10}$) was calculated in order to obtain the mesopore volume (V_{meso}) of the samples using the equation $V_{meso} = V_{net} - V_{0.10}$ (Fathy *et al*., 2010).

Ultra high resolution field emission scanning electron microscope (FESEM) was used to obtain images from the samples previously coated with platinum using a Zeiss Ultra plus FESEM. The FESEM was equipped with an energy dispersive spectrophotometer (EDS) Oxford Instruments INCA-X-act to analyze the elemental surface composition of the carbons. This analysis was carried out 5 times in different areas of the samples and the average was calculated.

Fourier transformed infrared spectroscopy with an attenuated transmitted reflectance accessory (FTIR-ATR), Shimadzu Prestige 21, was used in order to obtain the IR spectra for the activated carbon samples.

The Raman spectra have been obtained using a Horiba Jobin-Yvon LabRAM HR800, that is a high-resolution confocal μ-Raman system where the analysis area and depth can be limited down to one μm and two μm, respectively. The system is equipped with a 488 nm (visible) laser source. Structural analysis was carried out by X-ray diffraction (XRD) using a diffractometer Siemens D5000 operated at 30 KV and 20 mA, with CuKα radiation.

The pH of point of zero charge (pH_{PZC}) was determined based on the acid-base titration method. A 0.01 M solution of KNO_3 was prepared and bubbled with nitrogen to avoid the CO_2 effect; then the solution was divided in eight 250 ml flasks, each one with 50 ml of the solution. The pH level was adjusted in each flask to reach values between 3 and 10 using 0.1 M of NaOH and/or H_2SO_4 solutions. 0.1 g of the activated carbon samples was put into each flask and they were shaken for 48 h to reach the equilibrium. Then the activated carbon particles were filtered and the final pH was measured.

The pH_{PZC} was calculated from the interception between the curves $pH_{initial}$ vs pH_{final} and $pH_{initial}$ vs $pH_{initial}$. These measurements were done twice and the average was reported.

2.3 Adsorption test

2.3.1 Adsorption with methylene blue (kinetic and equilibrium test)

For the equilibrium experiments, different initial concentrations of methylene blue (MB) (Certistain C.I. 52015 - Merck) were prepared in the range between 40 and 120 mg/l from a starting solution of 1000 mg/l. A solution of 100 ml was put in separated 250 ml flasks and 50 mg of activated carbon (AC) was added. Samples were shaken at 180 rpm in an orbital shaker for 24 h at the constant temperature of 30±2 °C. The MB concentrations were determined on a Spectroquant Pharo 300 UV-VIS spectrophotometer (Merck) at the wavelength of 660 nm.

The removal of MB (%) at time t was calculated as follows:

$$Removal(\%) = \frac{C_i - C_t}{C_i} \times 100 \qquad (1)$$

where C_i is the initial concentration of MB and C_t is the concentration of MB at time t.

The Langmuir (1918) and Freundlich (1906) models were employed to test the equilibrium adsorption data of the adsorbents. The linear Langmuir isotherm equation is represented by the following equation:

$$\frac{C_e}{q_e} = \frac{1}{K_L q_{max}} + \frac{C_e}{q_{max}} \qquad (2)$$

where q_e is the amount of MB adsorbed at equilibrium time (mg/g), C_e is the equilibrium concentration of the adsorbed MB (mg/L), q_{max} and K_L are Langmuir constants related to maximum adsorption capacity (monolayer capacity) and energy of adsorption, respectively. Both q_{max} and K_L were calculated from the slope and the interception of the graphic C_e/q_e vs C_e, respectively.

The logarithmic form of Freundlich model is given by:

$$\log q_e = \log K_F + \frac{1}{n}\log C_e \tag{3}$$

where K_F can be defined as an adsorption or distribution coefficient and represents the quantity of adsorbate adsorbed onto AC for a unit of equilibrium concentration. The slope $1/n$ is a measure of the adsorption intensity or surface heterogeneity.

The MB kinetic experiments were conducted without a pH adjustment at room temperature. Two different types of experiments were conducted to study the effect of the initial MB concentration and the AC dose over the adsorption of the dye. In order to test the initial MB concentrations, solutions of 50, 100 and 150 mg/l (prepared from a starting solution of 1000 mg/l) of the dye were used with a constant AC dose (0.5 g/l) and AC particle size (fraction between 0.25 and 0.5 mm). In order to test the effect of activated carbon dosage, 0.25, 0.5, 0.75 and 1 g/l of the samples were used with a constant initial MB initial concentration (50 mg/l) and AC particle size (fraction between 0.25 and 0.5 mm). In both cases, the suspensions were mixed in a magnetic stirrer during the experiments. Liquid aliquots were extracted and filtered at the beginning and at different times between 5 and 240 min. The MB concentration was determined by the spectrophotometric method.

Two kinetic models were applied to describe MB adsorption data: the pseudo-first and pseudo-second order models. The pseudo-first order kinetic model can be represented by the equation:

$$\log(q_1 - q_t) = \log(q_1) - \frac{k_1}{2.303}t \tag{4}$$

where q_1 is the amount of adsorbate adsorbed at equilibrium (mg/g); q_t is the amount sorbed at time t (mg/g), and k_1 is the equilibrium rate constant of first order sorption (min^{-1}). The parameters k_1 and q_1 were calculated from the slop and the interception of the curve $\log(q_1 - q_t)$ vs t respectively.

The integrated form of the pseudo-second model can be written as follows (Ho and Mckay, 1999):

$$\frac{t}{q_t} = \frac{1}{K_2 q_e^2} + \frac{t}{q_e} \tag{5}$$

where t is the adsorption time (min), q_t is the amount of MB adsorbed at time t (mg of adsorbate/g of activated carbon), k_2 is the pseudo-second-order rate constant (g of adsorbent/mg of adsorbate·min) and q_e is the calculated equilibrium adsorption capacity (mg of adsorbate/g of activated carbon). The initial adsorption rate as q_t/t approaches 0, h (mg of adsorbate/g of adsorbent·min) was calculated according $h = k_2.q_e^2$ (Ho and Mckay, 1999). The kinetic parameters of this model were calculated from the plot of t/q_t as a function of time.

In order to calculated q_t the following equation was used:

$$q_t = \frac{(C_i - C_t)V}{m} \tag{6}$$

where C_i and C_t are the concentration of MB (mg/l) at the initial and at the time t respectively, V is the volume of MB solution (l) and m is the activated carbon dosage (g/l).

2.3.2 *Kinetic adsorption experiments with real polluted water with Pb and As*

A sample of polluted river water was taken from Tumbes river in northwest Peru. Acidification of water samples (pH<2) preserves most trace metals and reduces precipitation. Thus, immediately after the sample was taken, concentrated nitric acid was added to the river water to decrease its pH below 2. Water samples were filtered and the pH was adjusted to pH around 6 before the adsorption experiments, in order to be sure that the heavy metals remain dissolved in the water and avoid the precipitation effect. Initial heavy metals and minerals concentrations were analyzed to have a baseline for adsorption experiments.

Aliquots were taken at different times during the 300 min (0, 5, 10, 20, 40, 60, 90, 120, 180, 240 and 300) of the kinetic experiment with a syringe, and then were filtered to retain the activated carbon particles with a 0.2 μm filter, throwing the first 1 ml away to pre-saturate the filter with the sample water. Then 10 ml of the sample was acidified with nitric acid to be sure that the pH of the sample was lower than 3 and stored at 4 °C until the analysis.

Additionally, the content of others heavy metals and elements in the samples were analyzed at 300 min to compare this results with the full composition of the water at the initial time and examine the possible

adsorption those elements over the AC samples. As, Pb and others heavy metals and elements were detected by an Inductively Coupled Plasma Mass Spectrometer, Thermo Fisher Scientific, XSeries II QICP-MS.

3 Results and discussion

3.1 *Characterization of produced activated carbons*

Based on the nitrogen isotherms of both produced activated carbons (Fig. 1), the isotherm shape corresponded to type I according IUPAC classification (Gregg and Sing, 1982), which is basically characteristic of microporous materials. However, the slope of the linear branch increased slightly at higher relative pressure that suggests that there is a widening of the microporosity and a contribution of the mesoporosity (Texier-Madoki *et al*., 2004).

Both samples exhibit S_{BET} as high as 1278 and 1404 m^2/g for CSs and CCs, respectively. These levels of S_{BET} are comparable for wood sawdust based activated carbons obtained in others works: up to 914 m^2/g for sapelli wood sawdust AC (Thue *et al*., 2017), 1131 m^2/g for AC made of *Leucaena leucocephala* waste sawdust (Malwade *et al*., 2016), up to 788 m^2/g for pine sawdust AC (Durán *et al*., 2017), up to 1093 m^2/g for pine sawdust AC (Gao *et al*., 2017), between 782 and 2435 m^2/g in the case of paulownia sawdust AC, among others.

The proportion of micropore volume over total pore volume of the samples (V_{DR}/V_{net}) is 85.50 % and 95.20 % for CSs and CCs, respectively, which indicates that the adsorbents are predominantly microporous. Although the mesopore region is quite low in the activated carbons structure, CSs had slightly higher mesopore volume than CCs (Table 1).

The morphology structure of the sample CSs is mainly porous (FESEM images, Fig. 2a,b), with irregular pore sizes and shapes. Some impurities could be seen on the surface of the sample, which might be evolved from the chemical activator agent or other impurities that come from the same material after being grounded and sieved. The FESEM images of the sample CCs (Fig. 2c,d) show that it contains a well-developed pore structure, with different pore sizes and with circular and elliptical pore shapes. CCs surface is very clean, without impurities and its pore structure exhibits channeling-like pore morphology.

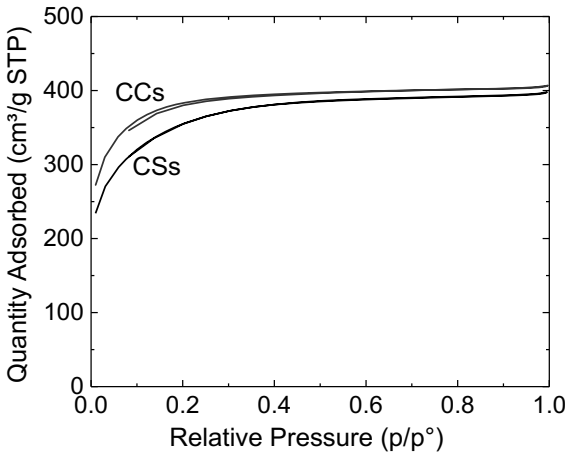

Fig. 1. Nitrogen adsorption isotherms (77 K) of the produced activated carbons.

Table 1. Textural properties of produced activated carbons.

Sample	S_{BET} (m^2/g)	V_{net} (cm^3_{liq}/g)	V_{DR} (cm^3_{liq}/g)	V_{DR}/V_{net} (%)	$V_{0.1}$ (cm^3_{liq}/g)	$V_{0.1}/V_{net}$ (%)	V_{meso} (cm^3_{liq}/g)
CSs	1278	0.62	0.53	85.5	0.5	80.7	0.12
CCs	1404	0.63	0.6	95.2	0.56	88.9	0.07

S_{BET} total surface area calculated by the classical BET model
V_{net} total pore volume obtained from the nitrogen adsorption at the maximum value of p/p_0 (~0.9900)
V_{DR} micropore volume determine by model Dubinin-Radushkevich equation
$V_{0.1}$ N_2 liquid volume at $p/p_0 = 0.1$.
V_{meso} mesopore volume ($V_{meso} = V_{net} - V_{0.10}$)

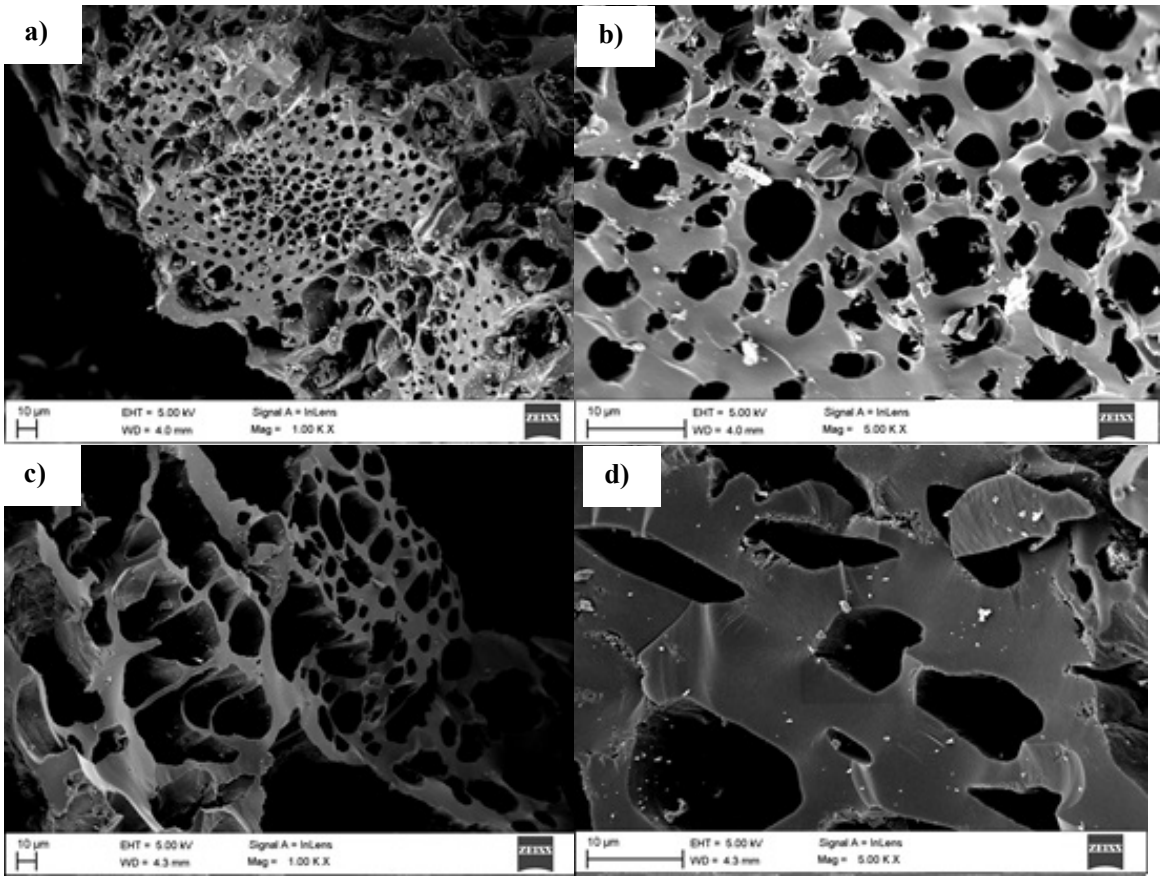

Fig. 2. FESEM images of the (a,b) *Colicodendron scabrida Ducke* activated carbon (CSs) and (c,d) *Cedrelinga catenaeformis* activated carbon (CCs).

Table 2. Parameters of the equilibrium models used to evaluate adsorption data.

Model	Parameter	CSs	CCs
Equilibrium models			
Langmuir	q_{max} (mg/g)	250	357
	K_L (l/g)	40	14
	R^2	0.999	0.984
Freundlich	K_F (mg/g)	302	864
	$1/n$	0.27	0.58
	R^2	0.813	0.955

For further information related to the impurities on the surface of the activated carbons, EDX analyze was conducted. Both samples content some impurities over their surface, *i.e.*, CSs has N, S and Zn in amounts higher than 1.5 %, while CCs has Cl in a proportion higher than 1%. The fact that CSs content significantly more impurities than CCs could affect negatively its adsorption capacity because of a reduction in the active sites over the surface of the activated carbon and the blockage of a portion of porous structure.

Based on FESEM micrographics, the sample CCs seems having more ordered pore structure than CSs, thus it might be easier for the sample CCs release the impurities evolved from the chemical activator during the wash step than the sample CSs.

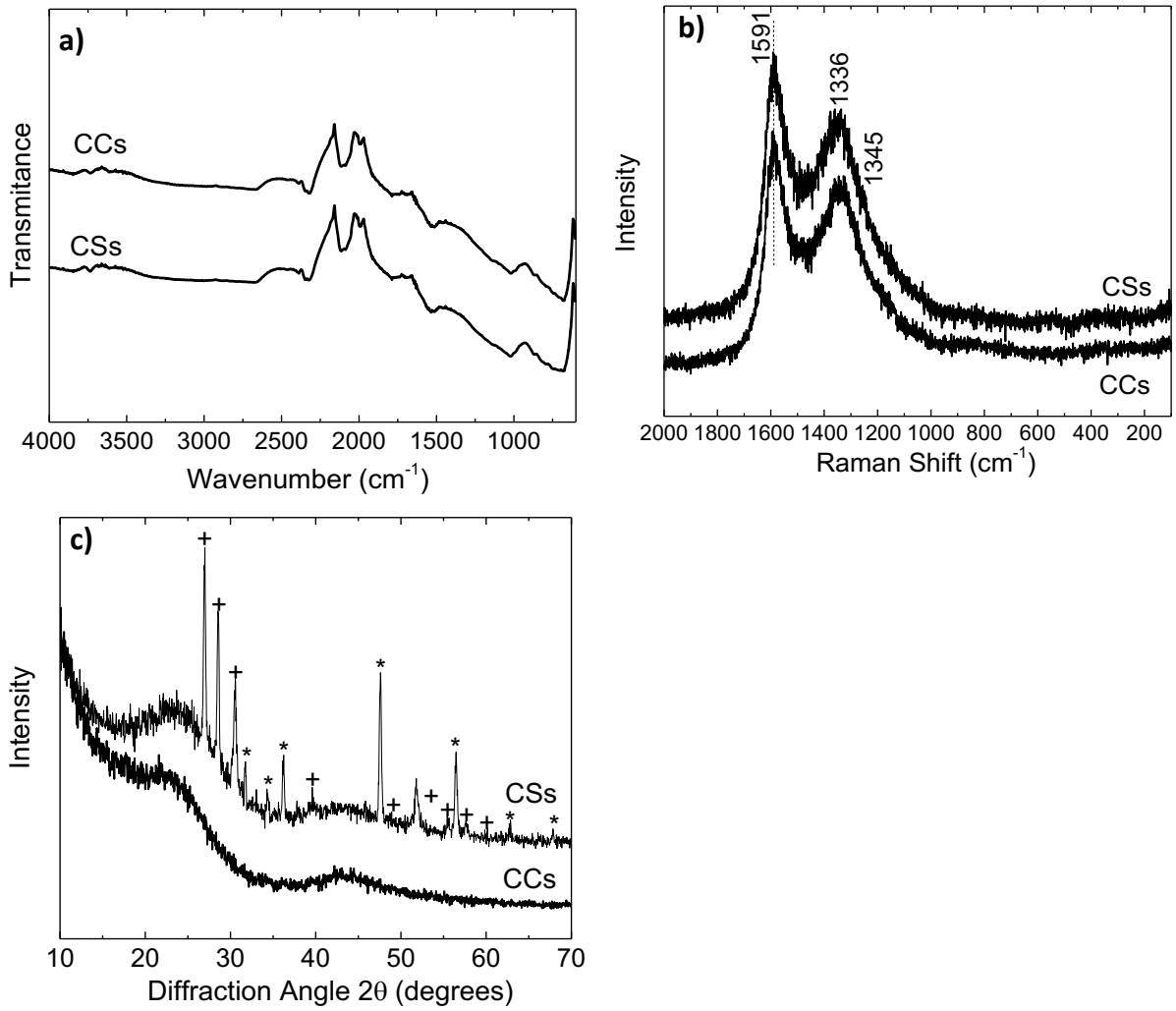

Fig. 3. FTIR-ATR spectra (a), Raman spectra (b) and X-ray diffraction analysis (c) of both produced activated carbons made of sawdust waste materials. In the case of X-ray diffractogram, peaks identify by * and + correspond to ZnO and ZnS phases.

FTIR-ATR spectra (Fig. 3a) of both activated carbon (AC) samples are very similar. Both ACs present a peak around 2100 cm^{-1} corresponding to C≡C vibrations in alkyne group (Alhamed *et al*., 2009). The bands close to 1525.6 cm^{-1} and 1531.4 cm^{-1} for CCs and CSs correspond to skeletal C=C vibrations in aromatic compounds (Sahu *et al*., 2010), C=O in the quinone structure (Tsai *et al*., 2001) and/or carboxylate groups (Oliveira *et al*., 2009). The peaks at 1026.2 and 1024.2 cm^{-1} for both samples CCs and CSc suggest the presence of C-O stretching vibrations that likely belong to alcohols, phenol, and ether or ester functional groups. Peaks around 678.9 and 675.1 cm^{-1} for the samples indicate O-H bending vibrations. The peak around 2318.4 - 2330 cm^{-1} for both activated carbon samples correspond to CO_2 effect.

Raman spectra (Fig. 3b) from both activated carbons show the presence of the D and G characteristic bands centered at 1336 cm^{-1} and at 1591 cm^{-1} for CSs sample, and centered at 1345 cm^{-1} and at 1591 cm^{-1} for CCs sample. That spectrum is common for the AC carbon structure (Chu and Li., 2006). This result and the fact that the carbonization of both raw materials was performed at relatively low temperature (600 °C) suppose that the amorphous character of the prepared carbon is dominating with respect to the nanocrystalline forms.

Table 3. Parameters of the kinetic model applied to MB adsorption data using both activated carbon samples. Effect of the initial MB concentration: 50, 100 and 150 mg/l.

Pseudo first order						
Parameter	CSs (50 mg/l)	CCs (50 mg/l)	CSs (100 mg/l)	CCs (100 mg/l)	CSs (150 mg/l)	CCs (150 mg/l)
q_{exp} (mg/g)	89.5	89.7	198.6	192.8	223.4	268.8
q_1	97.1	61.4	141.3	152.3	124.8	205.8
k_1 (min^{-1})	0.05	0.06	0.06	0.03	0.02	0.04
R^2	0.9922	0.9772	0.9456	0.9844	0.8509	0.9565
Pseudo second order						
Parameter	CSs (50 mg/l)	CCs (50 mg/l)	CSs (100 mg/l)	CCs (100 mg/l)	CSs (150 mg/l)	CCs (150 mg/l)
q_e (mg/g)	101.1	95.3	208.3	208.3	227.3	277.8
k_2 (g/mg.min)	0.0005	0.0013	0.0004	0.0006	0.0004	0.0004
h (mg/g.min)	6.3	14	16.8	26.1	19	27.8
R^2	0.979	0.995	0.996	0.9979	0.9969	0.9983

The ratio of intensity of the D-band to intensity of the G-band (I_D/I_G) is 0.84 for both samples indicating same grade of disorder on the structure of both activated carbons.

X-ray diffraction for both activated carbons (Fig. 3c) showed two asymmetric very broad peaks at around 24 and 42 degrees, which could be assigned to the planes (002) and (100) of the disordered graphite (Acharya *et al*., 2009) and are common for the activated carbon. The CSs sample has other peaks that correspond to ZnO and ZnS phases. The presence of zinc oxide and zinc sulfide in the surface of the CSs could be produced as impurities from the chemical activation since the chemical agent was $ZnCl_2$. This coincides with the high levels of Zn and S found in the samples CSs by EDX.

The CCs sample has not a crystalline phase that agrees with the FESEM images corresponding to the clean surface.

3.2 Adsorption experiments with methylene blue

3.2.1 Equilibrium experiments

For both CSs and CCs the MB equilibrium adsorption data fitted pretty well to the Langmuir model instead of Freundlich (Table 3) model. It supposes that the adsorption process between MB and the produced ACs is homogeneous in the monolayer.

Both samples showed maximum MB adsorption values close to 250 mg/g and 357 mg/g in the case of CSs and CCs, respectively (Table 3). According Cruz *et al*. (2015) the molecular size of methylene blue is 1.66 x 0.82 x 0.54 nm. Therefore MB blue could access the macro and mesoporous structure; however it depends on the position of the molecule to access partially the microporous structure. Since CSs has higher mesoporous pore volume than CCs, but lower maximum adsorption capacity of MB, mesoporous structure could not play the key parameter for the adsorption o MB by the produced AC. The key parameter might be the range of microporous structure where the MB is able to access and the order in the porous structure. In that case CCs has higher microporous structure and better disposition of pores according FESEM. Because in this study the micropore size distribution has not been studied, the better performance of CCs to adsorb MB is attributed to its larger specific surface area (1404 g/m^2).

The maximum MB adsorptions are comparable with that of AC produced from: rattan sawdust (294.14 mg/g) (Hameed *et al*., 2007a), olive-seed waste residue (190-263 mg/g), oil palm shell (243.90 mg/g), *Hevea brasiliensis* seed (227.27 mg/g), jute

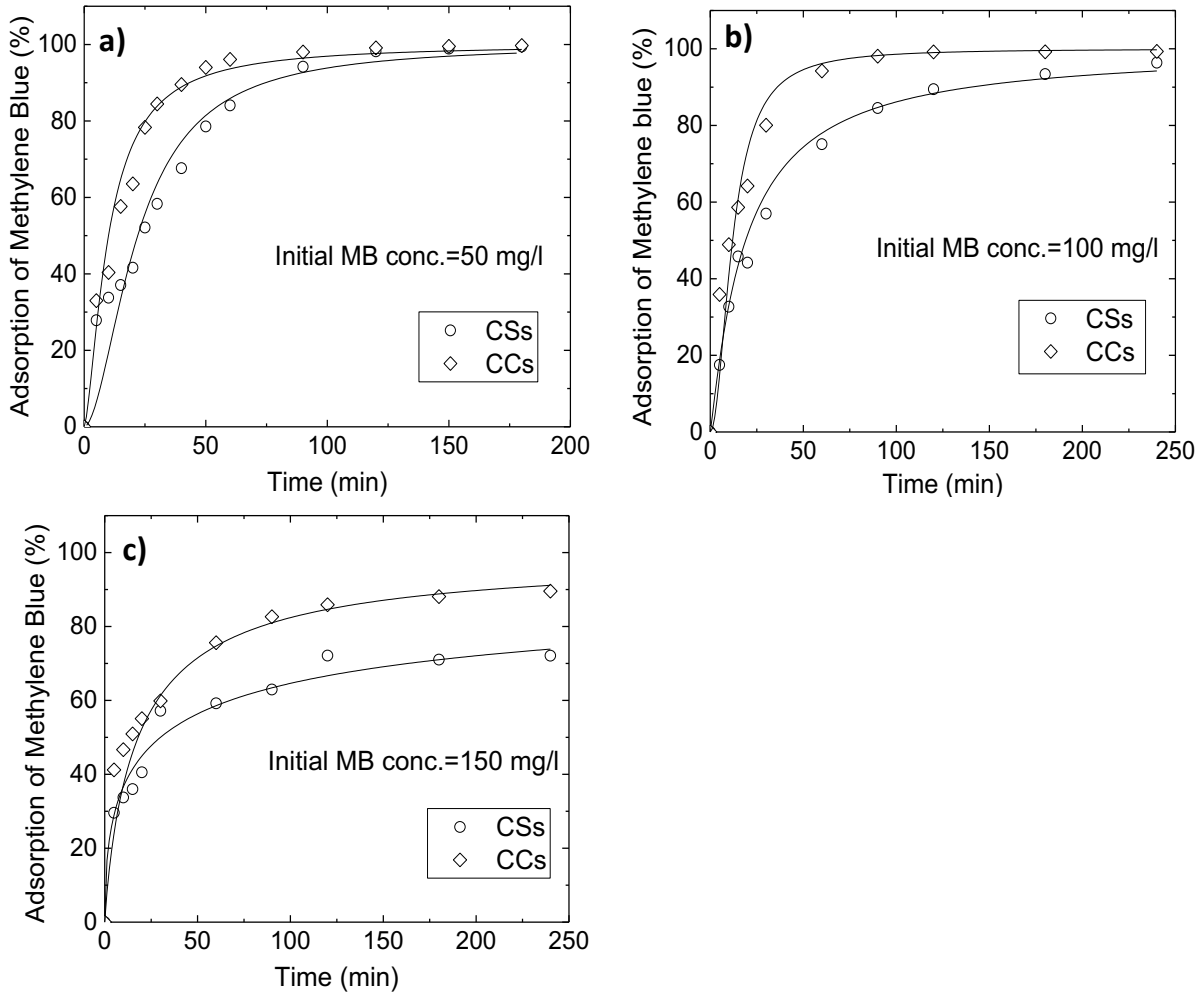

Fig. 4. Kinetic MB adsorption data and pseudo-second order model graphic for the adsorption data. Effect of the initial methylene blue concentration: 50, 100 and 150 mg/l. AC dosage = 0.5 g/l.

fiber carbon (225.64 mg/g), oil palm fiber (277.78 mg/g), coconut shell (277.90 mg/g), durian shell (289.26 mg/g), rice husk (343.50 mg/g), and vetiver roots (375 mg/g) (Rafatullah *et al*., 2010).

3.3 Kinetic experiments

The kinetic adsorption experiments indicate that the removal of MB was faster when the initial concentration of MB is lower (Fig. 4). When the AC dosage is constant and the initial concentration of the pollutant increases, the active sites of the AC are occupied faster, however there is a high amount of pollutant still without being adsorbed, then the removal of the pollutant (%) is lower.

For all MB initial concentrations, CCs exhibits higher levels of MB removal than CSs. The high initial concentration of MB increased the difference between the levels of MB removal for CCs and CSs. It was mainly based on the fact that CCs sample has higher S_{BET} than CSs.

In general, almost all kinetic adsorption data (Table 3) fitted well to a pseudo-second order model. The higher initial concentration of MB, the higher q_e and h, but the lower k_2. Increasing the initial concentration provides a powerful driving force to overcome the mass transfer resistance between aqueous and solid phases (Karagöz *et al*., 2008), reaching higher levels of equilibrium adsorption capacities and having higher initial adsorption rate.

Table 4. Parameters of the kinetic model applied to MB adsorption data using different activated carbon dosages.

Pseudo first order								
Parameter	CSs (dose g/l)				CCs (dose g/l)			
	0.25	0.5	0.75	1	0.25	0.5	0.75	1
q_{exp} (mg/g)	174.3	99.5	66	49.8	175.5	99.7	66.6	50
q_1	112.8	88.8	40.7	8.7	140.6	97	62.1	12.4
k_1 (min^{-1})	0.02	0.057	0.057	0.052	0.02	0.067	0.109	0.06
R^2	0.9392	0.9745	0.9352	0.759	0.9283	0.9745	0.9857	0.8022
Pseudo second order								
Parameter	CSs (dose g/l)				CCs (dose g/l)			
	0.25	0.5	0.25	0.5	0.25	0.5	0.25	0.5
q_e (mg/g)	178.6	104.2	68.5	50.3	181.8	104.2	68.1	50.6
k_2 (g/mg.min)	0.0004	0.0011	0.002	0.0136	0.0002	0.0011	0.0036	0.0091
h (mg/g.min)	13.1	11.9	9.5	34.2	8.2	11.6	16.8	23.3
R^2	0.9909	0.9976	0.9975	0.9998	0.9246	0.9968	0.9992	0.9997

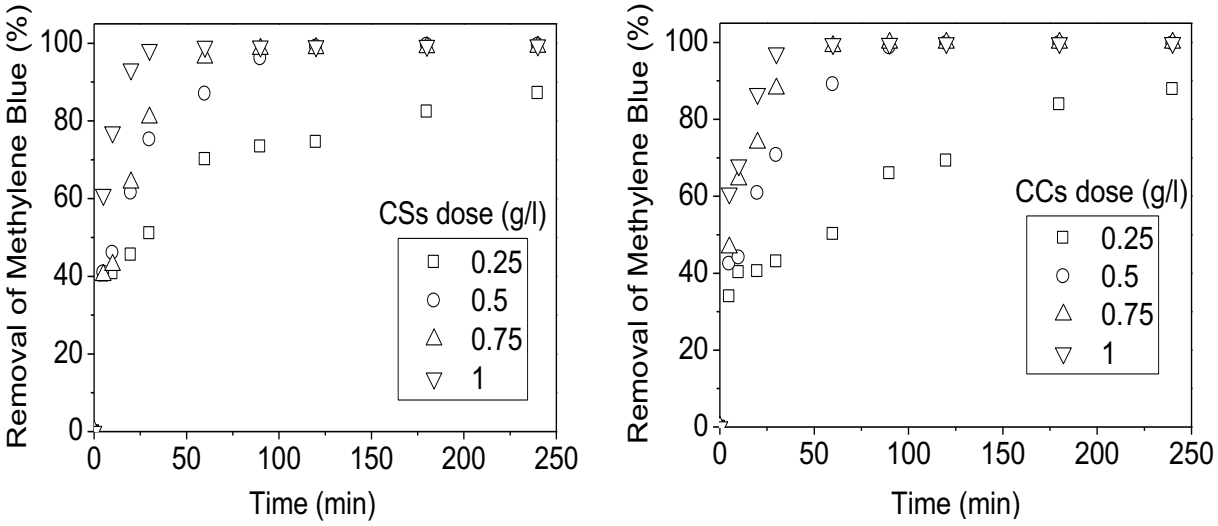

Fig. 5. Effect of the activated carbon dose over the removal of MB. Four activated carbon dosages were tested 0.25, 0.5, 0.75 and 1 g/l. Initial MB concentration = 50 mg/l.

Despite the R^2 of the pseudo-first model (0.9922) is higher than the R^2 of the pseudo-second order kinetic model (0.9790) for the sample CSs (50 mg/L), the fact that the amount of MB adsorbed at equilibrium calculated experimentally is widely different to the calculated by the model, indicates that it is not the correct model to fit the data.

Related to the effect of the initial AC dosage (Fig 5), as higher initial dose of AC is, as faster the equilibrium is reached. Obviously, keeping constant the MB initial concentration, if the AC dosage increases the amount of active sites is higher and the removal of MB is faster.

Table 5. Heavy metal content in the sample of water of the Tumbes River after 300 min of adsorption experiments compared with the initial concentration and the Peruvian water quality standard.

Element	Initial water (μg/l)	Concentration (μg/l) CSs	CCs	PWQS (*) (μg/l)
Al	1750	29.6	35.9	900
As	56.7	0.85	1.2	10
B	93	88.3	96.9	2400
Ba	72	71.3	69.2	700
Be	<0.1	<0.1	<0.1	12
Cd	2.2	0.5	1.4	3
Co	3.5	2.9	3.3	–
Cr	2.9	<0.4	<0.4	50
Cu	207	1.9	4.9	2000
Fe	2920	9.9	30.4	300
Hg	<0.2	<0.2	<0.2	1
Mn	229	218	218	400
Mo	0.5	0.64	0.43	70
Ni	4	2	2.7	70
Pb	224	1.3	2.3	10
Sb	10.9	8.8	8.9	—
Se	1.7	0.81	0.78	40
Sn	0.54	<0.2	<0.2	—
Tl	0.046	129	123	—
U	0.25	<0.02	<0.02	20
V	4.8	<0.3	<0.3	—
Zn	272	6430	921	3000

(*) Peruvian Water Quality Standards (SINIA, 2018)
— Not found

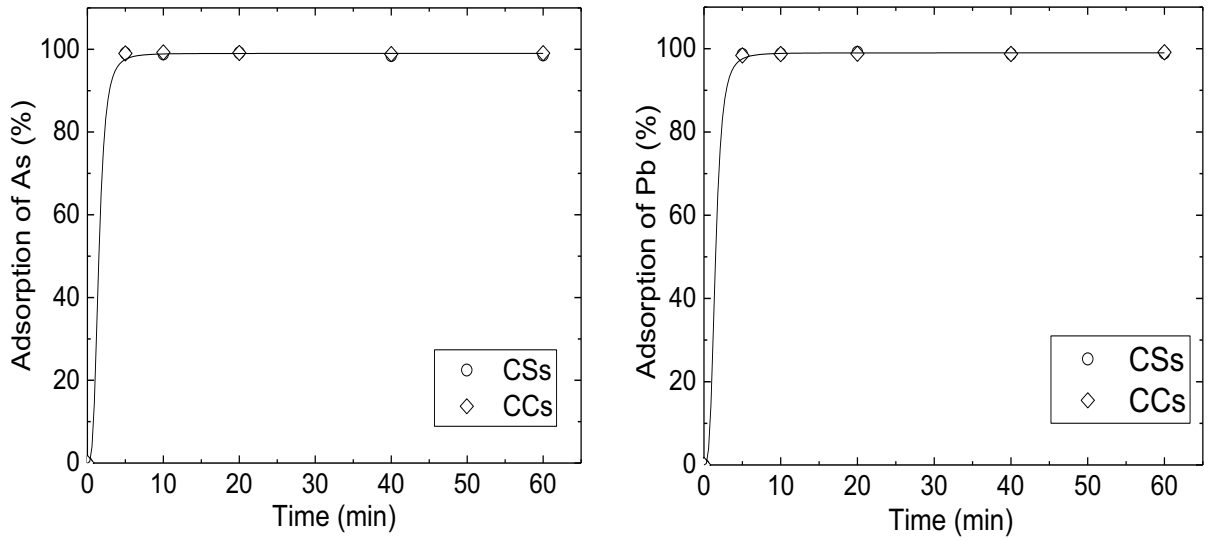

Fig. 6. Removal of As and Pb from water of the Tumbes river by both samples of activated carbon. The initial concentration of As and Pb in the polluted water was 57 and 224 μg/l respectively, while the activated carbon dosage 1 g/l.

In Table 4 is depicted the parameters of the two kinetic models used to fit the data. All data fitted the best to the pseudo-second order model (R^2 = 0.9246 - 0.9998). In the case of the sample CCs is clear than as higher the AC dosage is, the higher h is. However in the case of the sample CSs this fact does not occur at all. The explanation for that is related to the better disposition of pores in the sample CCs (easy access to the microporosity) and/or its less content of impurities (higher amount of impurities inside the pores can block it).

3.4 Adsorption experiments with polluted river water

The initial concentration of heavy metals and other elements present in the polluted river water before the adsorption experiments, the concentration of those after 300 min of experiments, as well as the Peruvian Water Quality Standards (PWQS) - category I: "Human consumption and recreational uses, subcategory A1: water that could be used for purification by disinfection" - SINIA (2018), are shown in the Table 5. The concentrations of As and Pb in the initial polluted river water exceed the PWQS; in the case of As its concentration surpasses the standards around 5.5 times, while Pb around 4.5 times. Besides As and Pb, the water from Tumbes river contains Al and Fe in sufficient concentrations to exceed PWQS.

The amount of the four elements mentioned above reduced until levels below their respective PWQS after 300 min of adsorption experiments with the produced ACs.

The initial concentration of elements such as Cd, Cu, Ni, Sb, Se, Sn, U and V did not surpass PWQS, however their concentration reduced as well after 300 min.

X-ray diffraction spectra indicated that CSs contained different compounds with Zn evolved from the chemical activation agent ($ZnCl_2$) and formed during the carbonization. This fact and the large contact time permit the Zn compounds, mainly ZnO located on the surface of the AC, to be transferred in the liquid phase, increasing the concentration of Zn in the aqueous phase.

The adsorption capacities of As and Pb by both produced ACs were very high, reaching levels close to 100 % for both pollutants even during the first 5 min of the adsorption experiment. For that reason only data within the first 60 min are showed in the Fig 6.

The pH behavior was similar during the adsorption experiments for both ACs. The pH level increased slightly from the initial pH 6 to a level no more than 6.5 in both cases. The experiments were carried out at pH levels slightly lower than the pH_{PZC} of both AC samples, 7.0±0.1 and 6.9±0.1 for CSs and CCs-AC, respectively. It means that the net charge of the AC would be positive, favoring the adsorption of As (V) which in the experimental condition of pH is present in the chemical form of oxyanions (Doušová *et al.*, 2003). Despite the net charge of the ACs surface is positive during the experiments, in the surface co-exist acidic and basic functional groups which are responsible for positive and negative charges (Boehm, 2002), allowing the adsorption of Pb cations as well.

Conclusion

Two activated carbons (ACs) were prepared from *Cedrelinga catenaeformis Ducke* and *Colicodendron scabrida* sawdust by chemical activation with $ZnCl_2$ (CCs and CSs, respectively).

Activated carbons with different qualities were obtained. The S_{BET} of the produced ACs was as high as 1278 and 1404 m^2/g for CSs and CCs, respectively. The pore structure of both activated carbons was predominantly microporous with the presence of mesopores.

Both samples exhibited similar functional groups in their surface and an amorphous character.

The pore surface of CCs is almost clean compared with the pore surface of the CSs, which exhibits impurities such as ZnO and ZnS evolved from the chemical activator and remnant in the solid phase.

Both samples showed maximum methylene blue (MB) adsorption equal to 250 mg/g in the case of CSs and 357 mg/g in the case of CCs, and the equilibrium MB adsorption data fitted well to the Langmuir model, supposing that the adsorption is homogeneous in the monolayer of the ACs.

The uptake capacity of As and Pb from the real polluted river water by both ACs were similar. They reached very high removal levels of both heavy metals close to 100% during the first 5 min, reducing the concentration of heavy metals until levels below the Peruvian Water Quality Standards. However based on the experiments, CCs is more suitable to water treatment applications.

Nomenclature

AC	activated carbon
C_0	initial concentration of adsorbate in solution (mg/l)
CCs	activated carbon derived from *Cedrelinga catenaeformis Ducke* sawdust
C_e	equilibrium concentration of the solute (mg/l)
CSs	activated carbon derived from *Colicodendron scabrida* sawdust
C_t	adsorbate concentration in solution at time t (mg/l)
FESEM	field emission scanning electronic microscope
FTIR-ATR	Fourier transformed infrared spectroscopy - attenuated total reflectance
h	initial adsorption rate as qt/t approaches 0 (mg/g·min)
k_2	pseudo-second-order rate constant (g/mg·min)
K_F	Freundlich constant related to the degree of adsorption
K_L	Langmuir constant (l/g)
MB	methylene blue
n	Freundlich constant related to intensity of the adsorption
pH_{PZC}	pH of zero point charge
PWQS	Peruvian water quality standard
q_e	calculated equilibrium adsorption capacity (mg/g)
q_{max}	maximum adsorption in the equilibrium state (mg/g)
q_t	amount adsorbed at time t (mg/g)
R^2	coefficient of determination of the specific model
S_{BET}	total surface area calculated by the classical BET model
SINIA	national system of environmental information (Peru)
$V_{0.1}$	N_2 liquid Volume at $p/p_0 = 0.1$
V_{DR}	micropore volume determine by model Dubinin-Radushkevich equation
V_{meso}	mesopore volume ($V_{meso} = V_{net} - V_{0.10}$)
V_{net}	total pore volume obtained from the nitrogen adsorption at the maximum value of p/p_0 (~0.9900)

Acknowledgements

The Academy of Finland is acknowledged for research funding to the AdMatU project (DNo: 269631) from the Development funds. The National University of Piura, the National University of Tumbes provided important financial support (Proyecto Canon - Resolución N° 0252-2016/UNT-R) and the Peruvian National Council for Science and Technology (CONCYTEC) (Contract N° 024-2016-FONDECYT) are gratefully recognized for their support.

References

Acharya, J., Sahu, J.N., Mohanty, C.R. and Meikap, B.C. (2009). Removal of lead (II) from wastewater by activated carbon developed from Tamarind wood by zinc chloride activation. *Chemical Engineering Journal 149*, 249-262

Alhamed, Y.A. and Bamufleh, H.S. (2009). Sulfur removal from model diesel fuel using granular activated carbon from dates stones activated by $ZnCl_2$. *Fuel 88* 87-94

Boehm, H.P. (2002). Surface oxides on carbon and their analysis: a critical assessment. *Carbon 40*, 145-149

Brunauer, S., Emmett, P.H. and Teller, E. (1938). Adsorption of gases in multimolecular layers. *Journal of American Chemical Society 60*, 309-319

Chu, P.K. and Li, L. (2006). Characterization of amorphous and nanocrystalline carbon films. *Materials Chemistry and Physics 96*, 253-277

Cruz, G., Pirilä, M., Huuhtanen, M., Carrión, L., Alvarenga, E. and Keiski, R.L. (2012). Production of activated carbon from cocoa (*Theobroma cacao*) pod husk. *Journal of Civil and Environmental Engineering 2*, 1-6

Cruz, G.J.F., Matějová, L., Pirilä, M., Ainassaari, K., Canepa, C.A., Solis, J., Cruz J.F., Šolcová, O. and Keiski, R.L. (2015). A comparative study on activated carbons derived from a broad range of agro-industrial wastes in removal of large-molecular-size organic pollutants in aqueous phase. *Water, Air, Soil Pollution 226*, 1-15

Doušová, B., Machovič, V., Koloušek, D., Kovanda, F. and Dorničák, V. (2003). Sorption of As (V) species from aqueous systems. *Water, Air, Soil Pollution 149*, 251-267

Durán, I., Rubiera, F., and Pevida, C. (2017). Separation of CO_2 in a solid waste management incineration facility using activated carbon derived from pine sawdust. *Energies 10*, 827.

Fathy, N.A., Girgis, B.S., Khalil, L.B. and Farah, J.Y. (2010). Utilization of cotton stalks-biomass waste in the production of carbon adsorbents by KOH activation for removal of dye-contaminated water. *Carbon Letters 11*, 224-234

Freundlich, H.M.F. (1906). Over the adsorption in solution. *Journal of Physics Chemistry 57*, e470

Gao, X., Wu, L., Li, Z., Xu, Q., Tian, W., and Wang, R. (2017). Preparation and characterization of high surface area activated carbon from pine wood sawdust by fast activation with H_3PO_4 in a spouted bed. *Journal of Material Cycles and Waste Management*, 1-12.

Gregg, S.J. and Sing, K.S.W. (1982). *Adsorption Surface Area and Porosity*. Academic Press, New York.

Hameed, B.H., Ahmad, A.L. and Latiff, K.N.A. (2007a). Adsorption of basic dye (methylene blue) onto activated carbon prepared from rattan sawdust. *Dyes Pigments 75*, 143-149

Hameed, B.H., Din, A.M. and Ahmad, A.L. (2007b). Adsorption of methylene blue onto bamboo-based activated carbon: kinetics and equilibrium studies. *Journal of Hazardous Materials 141*, 819-825

Ho Y.S. and McKay G. (1999). Pseudo-second order model for sorption processes. *Process Biochemistry 34*, 451-465

Ismadji, S., Sudaryanto, Y., Hartono, S.B., Setiawan, L.E.K. and Ayucitra, A. (2005). Activated carbon from char obtained from vacuum pyrolysis of teak sawdust: pore structure development and characterization. *Bioresource Technology 96*, 1364-1369

Karagöz, S., Tay, T., Ucar, S. and Erdem, M. (2008). Activated carbons from waste biomass by sulfuric acid activation and their use on methylene blue adsorption. *Bioresource Technology 99*, 6214-6222

Karthikeyan, T., Rajgopal, S. and Miranda, L.R. (2005). Chromium (VI) adsorption from aqueous solution by *Hevea Brasilinesis* sawdust activated carbon. *Journal of Hazardous Materials 124*, 192-199

Langmuir I. (1918). The adsorption of gases on plane surfaces of glass, mica and platinum, *Journal of American Chemical Society 40*, 1361-1403

Malarvizhi, R. and Sulochana, N. (2008). Sorption isotherm and kinetic studies of methylene blue uptake onto activated carbon prepared from wood apple shell. *Journal of Environmental Protection Science 2*, 40-46

Malwade, K., Lataye, D., Mhaisalkar, V., Kurwadkar, S., and Ramirez, D. (2016). Adsorption of hexavalent chromium onto activated carbon derived from *Leucaena leucocephala* waste sawdust: kinetics, equilibrium and thermodynamics. *International Journal of Environmental Science and Technology 13*, 2107-2116.

Mohanty, K., Das, D. and Biswas, M.N. (2005). Adsorption of phenol from aqueous solutions using activated carbons prepared from *Tectona grandis* sawdust by $ZnCl_2$ activation. *Chemical Engineering Journal 115*, 121-131

Oliveira, L.C., Pereira, E., Guimaraes, I.R., Vallone, A., Pereira, M., Mesquita, J.P. and Sapag, K. (2009). Preparation of activated carbons from coffee husks utilizing $FeCl_3$ and $ZnCl_2$ as activating agents. *Journal of Hazardous Materials 165*, 87-94

Rafatullah M., Sulaiman O., Hashim R. and Ahmad A. (2010). Adsorption of methylene blue on low-cost adsorbents: a review. *Journal of Hazardous Materials 177*, 70-80

Rao, M.M., Ramesh, A., Rao, G.P.C. and Seshaiah, K. (2006). Removal of copper and cadmium from the aqueous solutions by activated carbon derived from *Ceiba pentandra* hulls. *Journal of Hazardous Materials 129*, 23-129

Sahu, J.N., Acharya, J. and Meikap, B.C. (2010). Optimization of production conditions for activated carbons from tamarind wood by zinc chloride using response surface methodology. *Bioresource Technology 101*, 1974-1982

SINIA - Sistema Nacional de Información Ambiental (2018). Decreto Supremo N° 004-2017-MINAM.- Aprueban Estándares de Calidad Ambiental (ECA) para Agua y establecen Disposiciones Complementarias. http://sinia.minam.gob.pe/download/file/fid/59020. Accessed 04 February 2018

Srinivasakannan, C. and Bakar, M.Z.A. (2004). Production of activated carbon from rubber wood sawdust. *Biomass Bioenergy 27*, 89-96

Texier-Mandoki, N., Dentzer, J., Piquero, T., Saadallah, S., David, P., Vix-Guterl, C. (2004). Hydrogen storage in activated carbon materials: role of the nanoporous texture. *Carbon 42*, 2744-2747

Thue, P. S., dos Reis, G. S., Lima, E. C., Sieliechi, J. M., Dotto, G. L., Wamba, A. G., Dias S.L.P. and Pavan, F. A. (2017). Activated carbon obtained from sapelli wood sawdust by microwave heating for o-cresol adsorption. *Research on Chemical Intermediates 43*, 1063-1087.

Tsai, W.T., Chang, C.Y., Lin, M.C., Chien, S.F., Sun, H.F. and Hsieh, M.F. (2001). Adsorption of acid dye onto activated carbons prepared from agricultural waste bagasse by $ZnCl_2$ activation. *Chemosphere 45*, 51-58

Velázquez-Trujillo, A., Bolanos-Reynoso, E., and Pliego-Bravo, Y. S. (2010). Optimización de la producción de carbón activado a partir de bambú. *Revista Mexicana de Ingeniería Química 9*, 359-366.

Zhu, X. L., Wang, P. Y., Peng, C., Yang, J., and Yan, X. B. (2014). Activated carbon produced from paulownia sawdust for high-performance CO_2 sorbents. *Chinese Chemical Letters 25*, 929-932.